TD-09-003

FNAL March 12, 2009

HINS Linac SS2 Section Prototype Focusing Lens Design

G. Davis, T. Page, M. Tartaglia, I. Terechkine, J. Tompkins, T. Wokas

I. Introduction

Solenoid-based focusing lenses for the SS2 section of the HINS linac will be installed inside a cryomodule with SS2 superconducting spoke cavities. The requirements for these lenses are summarized in the table below.

Bore diameter	30 mm;
Required squared magnetic field integral	580 T^2-cm;
Current margin	~25%;
Available slot length	less than 294 mm;
Integrated strength of steering dipoles	0.5 T-cm.
Fringe field on the walls of cavities	less than 10μT

For each SS2 section, four lenses without embedded steering dipoles (Type-1) and two lenses with steering coils (Type-2) are needed. At present, only one SS2 section is within the scope of the HINS R&D program: in total, (including spares) five Type-1 and three Type-2 production solenoids must be built.

The design approach is quite similar to that employed for the SS1 system [1]: one solenoid design will be used with an optional steering dipole assembly installed inside the Type-2 systems.

II. Focusing Lens Design

Superconducting strand

Rectangular 1 x 0.6 mm^2 54-filament NbTi strand, made by Oxford Instruments, was selected for the main coil of the solenoid, The reasons for this decision included the decreasing availability of SSC-type strand and the need to simplify quench protection issues by making the inductance of the coil lower. We had experience using this strand earlier during the test solenoid program [2], and there was enough strand left from this exercise to make an SS2 prototype solenoid. The strand parameters are shown below:

- Bare strand dimensions	1.015 mm x 0.60 mm;
- Insulated strand dimensions	1.08 mm x 0.66 mm;
- Bare strand cross-section	0.604 mm^2;
- Cu/non-Cu ratio	1.35
- Number of filaments	54
- Filament diameter	70 μm;

Results of critical current measurement of the strand are shown in Table 1:

Table 1: Critical surface of the rectangular 1.0 x 0.6 mm strand at 4.20 K

B (T)	6	7	8	9
Ic (A)	546	418	290	162

For the solenoid bucking coils , Oxford 0.5 mm round NbTi strand is used, as it was for the SS1 program. Parameters of this strand are shown below:

- Bare strand diameter 0.5 mm;
- Insulated strand diameter 0.525 mm;
- Bare strand cross-section 0.196 mm^2;
- Cu/non-Cu ratio 1.3
- Number of filaments 54

Results of critical current measurement of the strand are shown in Table 2:

Table 2: Critical surface of the round 0.5 mm strand at 4.20 K

B(T)	3	4	5	6
Ic (A)	367	307	254	201

The correctors (steering dipoles) will be wound using 0.3 mm (bare diameter) strand 54S43 made by Supercon, Inc. The strand has a Cu/nonCu ratio of 1.3 and a 25 μm filament diameter. Table 3 shows the critical current of the strand versus applied field as specified by the vendor.

Table 3: Critical surface of 54S43 strand at 4.2 K

B (T)	3	5	7	9
I (A)	100	80	45	16

Solenoid Design

The main features of the solenoid design are shown in Fig. 1.

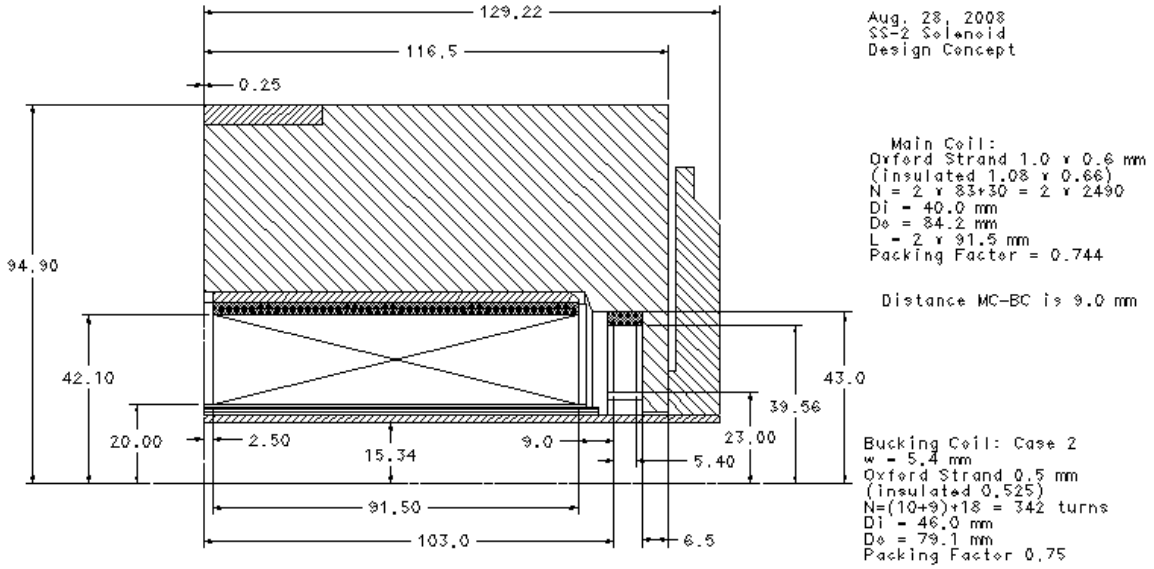

Fig. 1. SS2 focusing solenoid design.

The SS2 design is similar to that of the SS1 solenoid; the major difference is that the longer main coil is split into two coils separated by an insulating wall. This arrangement requires extra pair of leads, but allows more options for quench detection and protection;

e.g., it can simplify protection by making possible a ground connection in the middle of the main coil. The main coil has a total of 4980 turns; the inductance of the main coil is ~0.35 H.

The design of the bucking coils (BC) was also modified due to the change in the main coil strand cross-section. We expect a higher current in the bucking coils now, and they must be made thinner to provide the required bucking field. The BC-s cross-section height and position must also be adjusted for optimal field compensation. A different strand design was considered, but there was none available with the appropriate combination of strand diameter and performance.

The quench diagram of the device is shown in Fig. 2. In the main coil, the expected quench current is ~254A at 4.2 K; it is ~257A in the bucking coils. This situation can result in more quenches in the bucking coils during training and requires a quench protection scheme that ensures quick energy removal if a quench develops in the bucking coils.

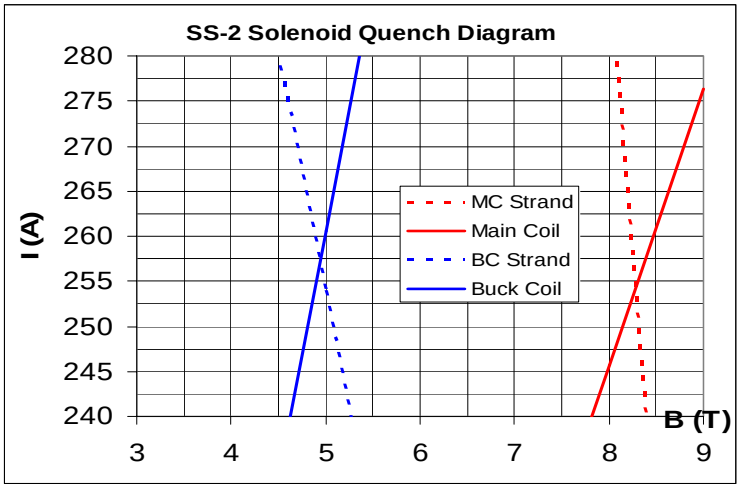

Fig. 2. SS2 solenoid quench diagram at 4.2 K.

The solenoid field distribution at 250A is shown in Fig. 3. The lower field in the center of the solenoid is due to the 5 mm thick separator plate that splits the main coil.

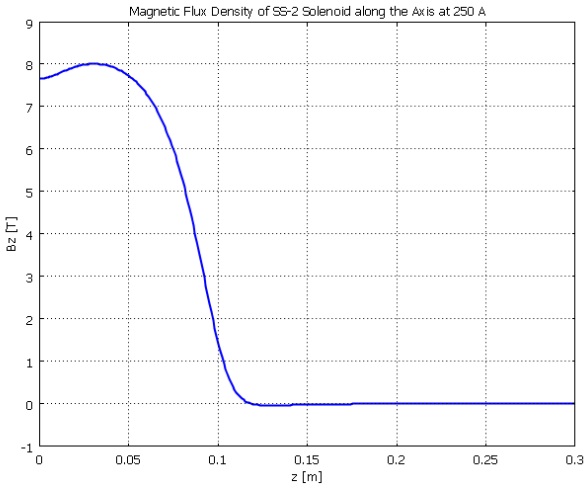

Fig. 3. Longitudinal profile of the magnetic field in the SS2 focusing solenoid at 250 A.

The squared field integral at 250A is 10.15 T^2-m. The nominal value of the integral of 5.8 T^2-m is reached at 189 A, so the current margin at 4.2 K is ~32%.

Conditions during solenoid testing in the updated MTF Stand 3 dewar or during normal operation in the planned cryomodule of the HINS linac, typically result in higher He temperatures than 4.2K reference value. During the testing of similar devices on Stand 3, the temperature was ~4.4 K, and it can be as high as 4.6 K in the cryostat. A higher operating temperature, of course, results in a lower critical current and must be taken into consideration in determining the magnet current margin. Fig. 4 compares critical current of the strand in the main coil of the solenoid for T = 4.2 K and T = 4.6 K. The quench at 4.6 K is expected at ~238 A. This value corresponds to a margin of ~23 % above the critical current.

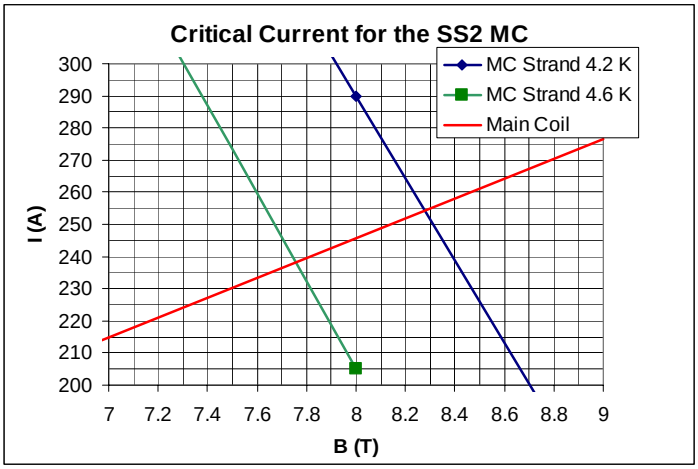

Fig. 4. SS2 MC quench current at 4.2 K and at 4.6 K.

Similarly, we have taken into account the higher operating temperature in the design of the bucking coils (Fig. 5): the expected quench current at 4.6 K is ~240 A, which is higher than that of the main coil.

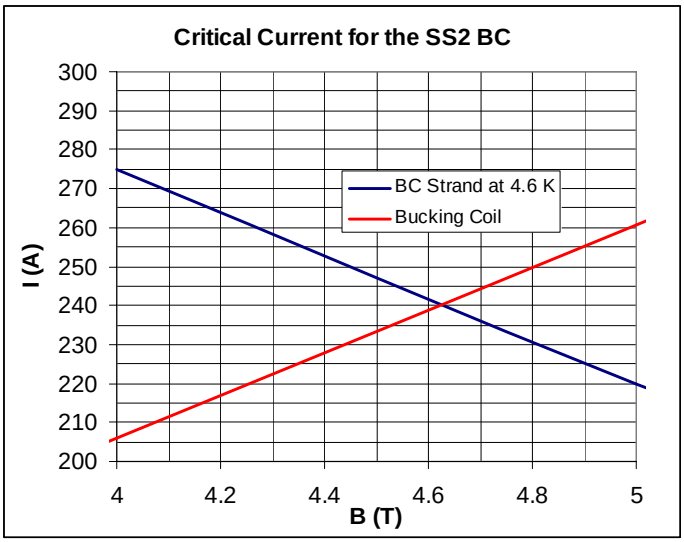

Fig. 5. SS2 BC quench current at 4.6 K.

We need to mention here that the predicted strand performance depends on the model of strand behavior employed; using different parameterizations of the critical surface can result in somewhat different predicted temperature dependence.

During the magnetic modeling stage, the fringe magnetic field was first tuned without using an additional magnetic shield. This was done by making fine adjustments of the number of layers in the bucking coils and by moving the cross-section of the coil radially and longitudinally. This tuning resulted in an optimized set of parameters for the bucking coils which was acceptable for the solenoid design: Rin = 23 mm, H = 16.56 mm; W = 5.4 mm; Z0 = 103 mm, N = 342; K_bc = 0.75. The graph of the expected fringe field (without shielding) is shown in Fig. 6.

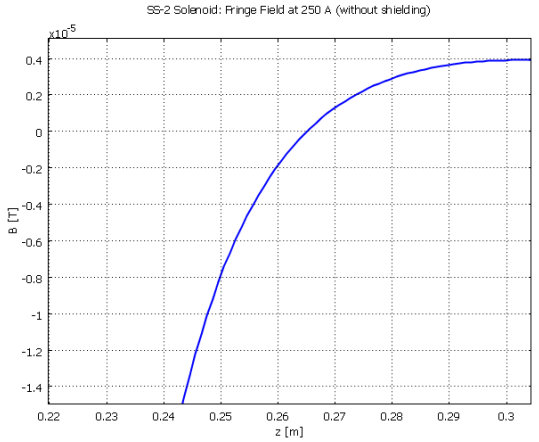

Fig. 6. Expected fringe field of the SS2 lens.

This level of fringe field meets specifications, [3] even without additional shielding. However, at these small field levels, the impact of small variations in fabrication can be significant, and the use of additional magnetic shielding is necessary.

Steering Dipoles

The design of the steering dipoles for the SS2 section solenoids is similar to that of the SS1 section solenoids, although they are longer. The cross-section of the dipole corrector assembly is shown in Fig. 7.

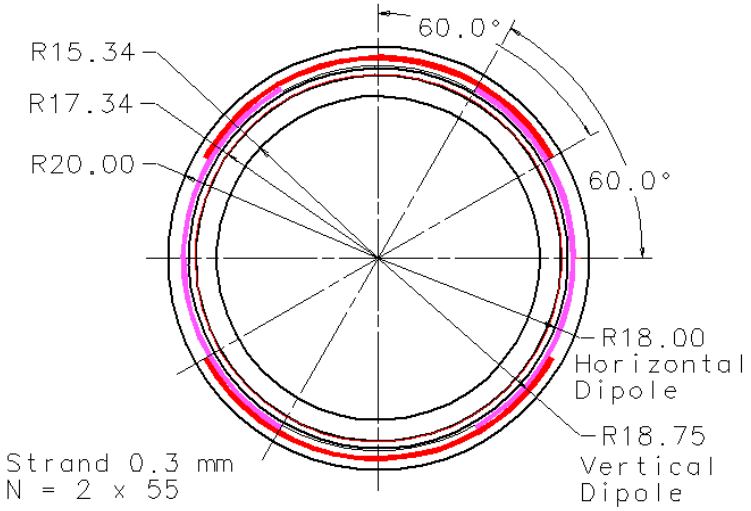

Fig. 7. Cross-section of the dipole corrector assembly.

The windings of the dipoles, which are made similar to that of the SS-1 solenoid steering dipoles (see [1] for more details), is laid out on a plane sheet of pre-impregnated fiberglass cloth. The sketch in Fig. 8 shows one-fourth of one of two winding that form one steering dipole – horizontal or vertical.

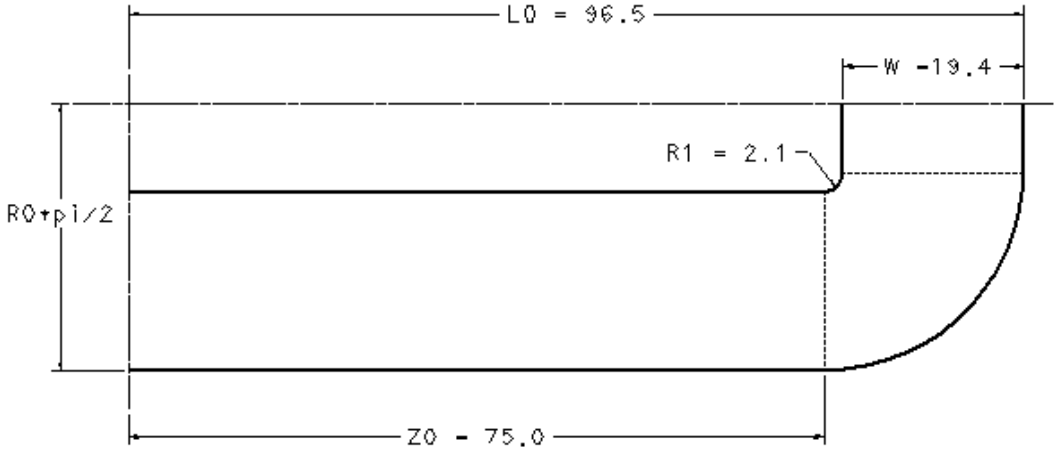

Fig. 8. Steering dipole winding layout.

The windings are then wrapped around the cylindrical surface of a thin-wall stainless steel spool, which forms a base for the windings. The height H of the profile is equal to one quarter of the base cylinder perimeter, $H = R_0 \cdot \pi/2$, where R_0 is the radius of a base cylinder of the winding. The horizontal and the vertical windings have slightly different inner radii, but the same number of turns. The base cylinder radius of R_0 = 18.5 mm is used for further field quality modeling; it is the average of the two steering dipoles center radii. The length of the winding straight section is Z_0 = 75 mm. The width of the winding is defined by the insulated strand diameter (0.33 mm), the number of turns (55), and the density of the winding; in our case this width W = 19.4 mm. The inner radius of the winding in the transition area is made R1 = 2.1 mm (Fig. 8). Fig. 9 shows a sketch of the corrector winding after it is formed into a cylinder.

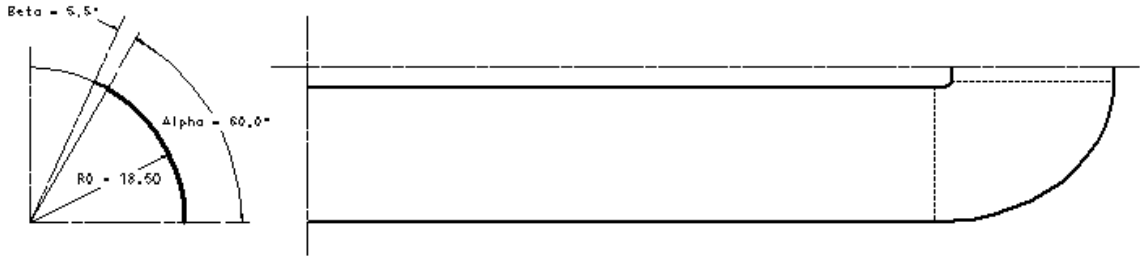

Fig. 9. The longitudinal profile of a steering dipole of the SS2-T2 solenoid.

Each winding is made in accordance with an optimized one-layer dipole configuration occupying the area on the surface between -60º and +60 º. Fiberglass insulation is used between the spool and the horizontal corrector and between the horizontal and the vertical corrector. The corrector assembly is placed inside a thin-wall G-10 cylinder that forms the base for winding the main coil of the solenoid. It is then impregnated with epoxy to form a rigid structure.

Modeling of the magnetic field of the steering dipole was made using a 3D surface current density approach. In this method, the current density on the surface of a base cylinder was assigned using logical expressions:

Jz = J0*(z<=Z0)*(y<=(R0*sin(Alpha))) +
Jz2*(z>Z0)*(rad<=(R1+W))*(y<=R0*sin(Alpha+Beta)) ;

Jx = Jx2*(z>Z0)*(rad<=(R1+W))*(y<=R0*sin(Alpha+Beta)) -
J0*y/R0*(z>(Z0+R1))*(z<L0)*(y>R0*sin(Alpha+Beta)) ;

Jy = Jy2*(z>Z0)*(rad<=(R1+W))*(y<=R0*sin(Alpha+Beta)) +
J0*x/R0*(z>(Z0+R1))*(z<L0)*(y>R0*sin(Alpha+Beta)) ;

In these expressions:

Jx2 = Jphi2*y/R0,
Jy2 = Jphi2*x/R0,
Jphi2 = J0*sin(Phi),
Jz2 = J0*cos(Phi),
Phi = asin((z-Z0)/rad),
rad = sqrt(rad_Y^2 + (z-Z0)^2),
rad_Y = R0*(Alpha+Beta-Psi),
Psi = asin(y/R0).

The angle Alpha = 60º (Fig. 9) defines the field quality and Beta = 6.5º is a function of the initial corner radius R1 = 2.1 mm (Fig. 8).

The area where the surface current exists is shown in red in Fig. 10. At any point on the surface, the current is made tangent to the spatial direction of the current-carrying strand.

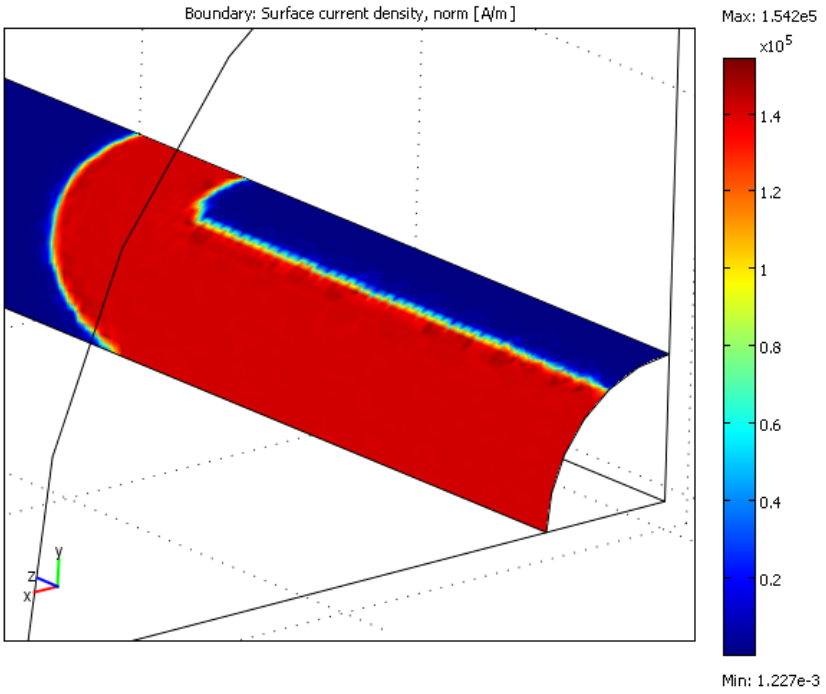

Fig. 10. Current distribution in the steering dipoles.

The expected distribution of the magnetic field of the horizontal steering dipole (in this case B_y) for four lines parallel to the z-axis of the solenoid (one along the axis, and three at the radius R = 15 mm: φ = 0º, φ = 90º, and φ = 45º) at 50 A without the solenoid flux return is shown in Fig. 11.

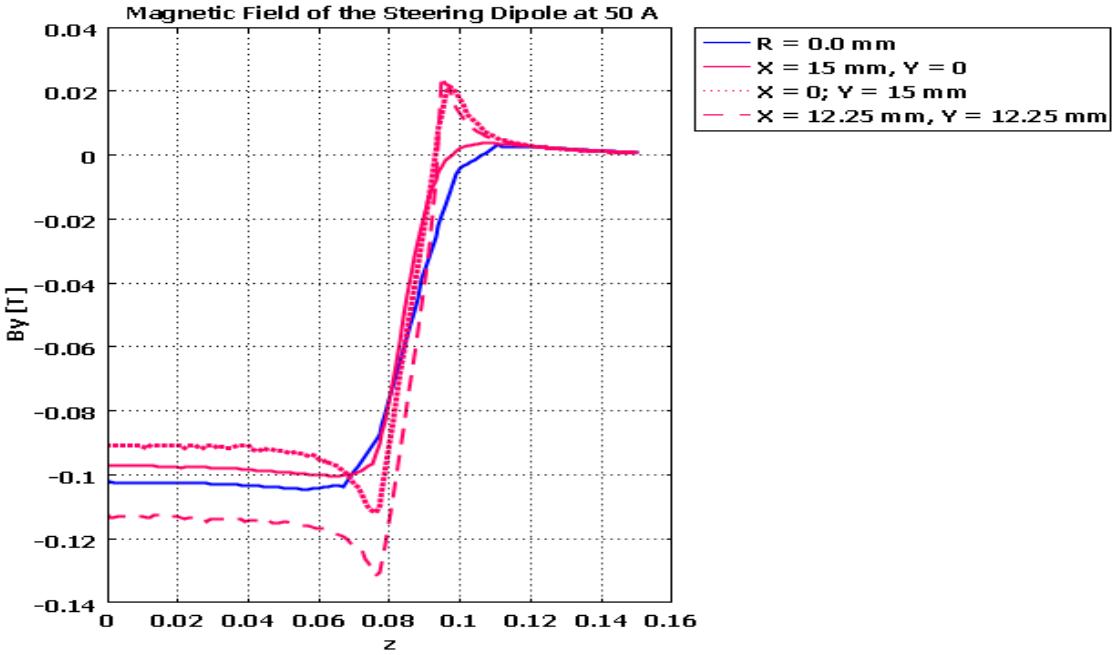

Fig. 11. Vertical magnetic field distribution in the steering coil, without a flux return.

Fig. 12 shows a color-coded vertical magnetic field map of the horizontal steering dipole in the cross-sections at z = 20 mm, z = 50 mm, and z = 80 mm for the same case with I = 50 A. The field is oriented in the negative Y direction. At z = 80 mm, the field starts to drop because this section is already in the transition region.

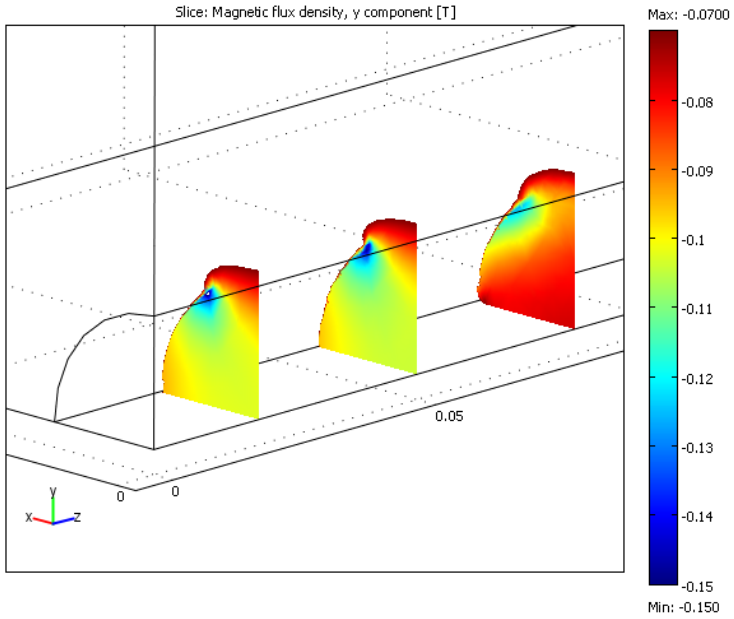

Fig. 12. Vertical magnetic field strength at z = 20, 50, and 80 mm, with no flux return.

Because the surface of the flux return is quite far from the solenoid, we do not expect significant change in the field distribution after the flux return is added. Corresponding plots are shown in Fig. 13 and Fig. 14. We see ~10% increase in the field strength due to the presence of the flux return.

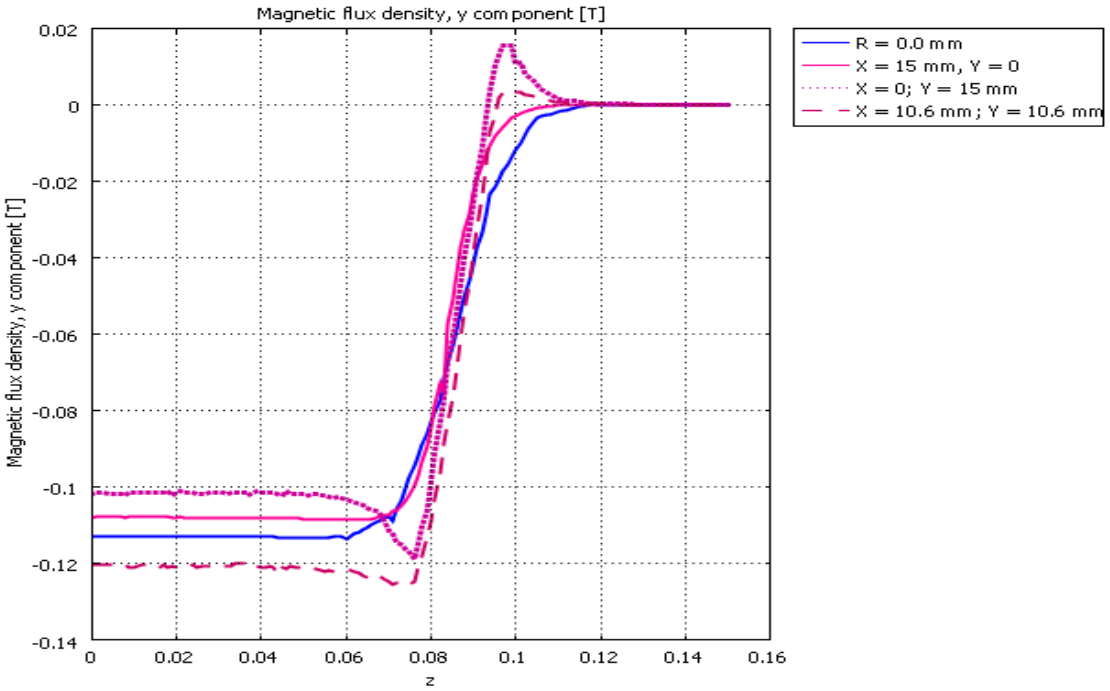

Fig. 13. Vertical magnetic field distribution in the steering coil, with the solenoid flux return installed ($\mu = 500$).

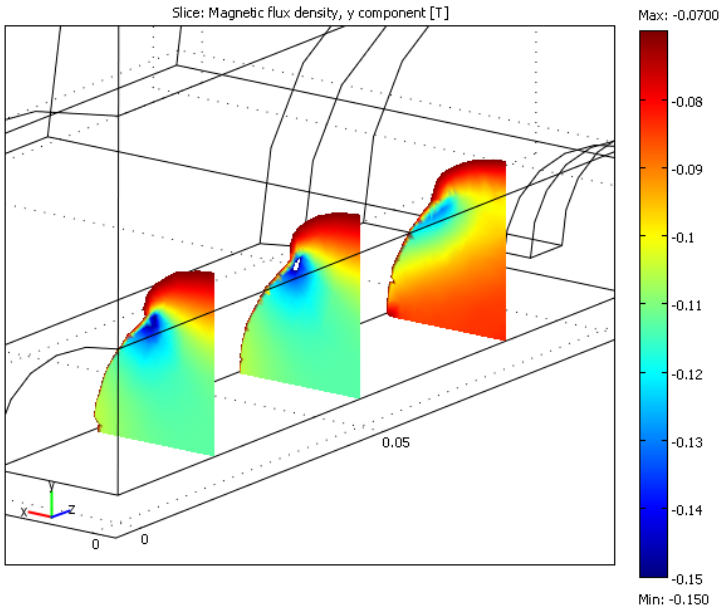

Fig. 14. Magnetic field map at z = 20, 50, and 80 mm, with the solenoid flux return installed ($\mu = 500$).

For the steering dipoles we also need to know the uniformity of the integrated strength across in the beam cross-section. On the axis, at 50 A, the integral of the vertical magnetic field over one half of the Z axis (0 to 150 mm) is 0.978 T-cm, which is significantly higher that the required 0.25 T-cm (full length integral 0.5 T-cm). As was done in [1], we have studied the bending integral uniformity in the beam pipe cross-section, relative to the on-axis field, ***Bya***:

$$\frac{dB_y}{B_y} = \frac{\int (By - Bya)dz}{\int (Bya)dz}$$

The lines along which the integrals were calculated are parallel to the solenoid axis and positioned at the radii R = 10 mm and R = 15 mm, at the angles φ = 0º, 45º, and 90º. The data for the integrated field uniformity are shown in Table 4.

Table 4: Field integral uniformity.

Radius \ Angle	0º	45º	90º
0 mm	0	0	0
10 mm	-0.013	+0.015	-0.019
15 mm	-0.059	+0.075	-0.098

The data in the table are quite comparable with the data in the Table 6 of [1] made for the SS1 solenoid. The field integral is uniform within 2% for R < 10 mm. It is uniform within 10% for R < 15 mm.

In [4] the measured SS1 solenoid corrector quench current was compared with the prediction while taking into account slightly elevated temperature during test due to pressure build in the test Dewar; the measured and the expected currents were within 5% from each other. Because strand used for the SS2 solenoid correctors is the same that was used for the SS1 solenoid correctors, expected quench current in the presence of the magnetic field of the solenoid must also be the same.

III. Solenoid Protection

Quench protection of SS2 section solenoids was studied in [5]. As shown in [6] and [7], it is possible to protect the quenching solenoid by adding a dump resistor to the current discharge circuit. The maximum voltage to ground, in the case when the quench occurs in one of the bucking coils, depends on the initial current in the circuit and on the value of the dump resistor. The graph in Fig. 15 illustrates the optimal value (1.75 Ohm) of the dump resistor at 200 A, which is close to the operating current. With this resistor in the circuit, the maximum voltage to ground is ~350 V. This voltage develops due to the appearance of the normal phase in the quenching superconducting coil and as an inductive reaction due to decay of the current. It has its maximum in the initial stage of the quench, when current is still high, but its derivative is already significant. Fig. 16 combines two graphs: the current and the maximum voltage traces when the quench occurs in a bucking coil in the case without a dump resistor in the circuit.

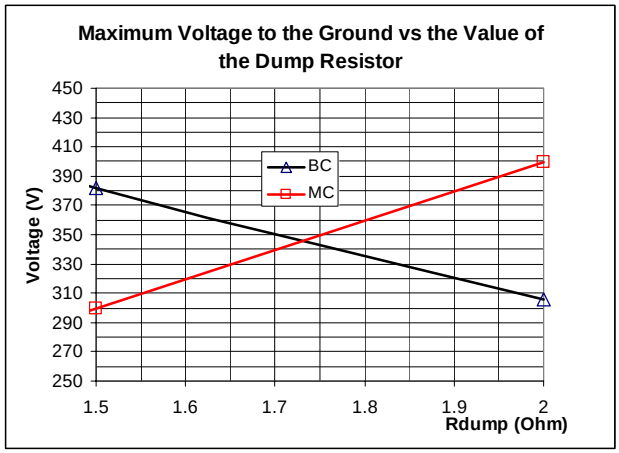

Fig. 15. Maximum voltage to ground after quenching in the SS2 solenoid BC.

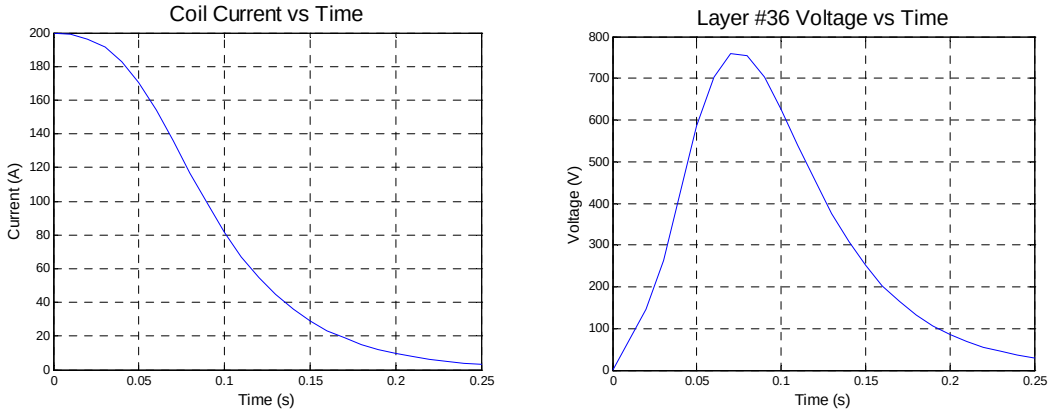

Fig. 16. Current and maximum voltage to ground in the SS2 solenoid during quench; I0 = 200 A, Rdump = 0.

Taking the optimal current discharge scheme described in [6], in the case when the value of the dump resistor is small, the area where the maximum voltage develops is between the main and the bucking coil. In the case when the dump resistor has optimal or higher value, the maximum voltage spot is between the main coil and the dump resistor. The voltage graph in Fig. 15 shows that there is a danger of a breakdown in the coil if no dump resistor is used, so it must be used every time.

With the initial current of 200 A and without using a dump resistor, the temperature in the quenching coil reaches ~260 K. With the optimal dump resistor it is ~ 170 K.

The situation becomes more critical if higher current is used, e.g. 250 A, as in the case of quench training. Just by using a dump resistor technique, it is impossible to make the voltage to ground lower than 600 V (see [5] for details). Without a dump resistor, the voltage can go as high as 1200 V and temperature in the coil can exceed 360 K, which significantly increases chances of irreversible damage during quenching. Additional protection measures must be developed for safe operation above the nominal current, as was indicated in [5].

IV. Conclusion

This study was made to propose a design concept of a focusing solenoid for the SS2 section of the HINS linac. The design was developed based on the experience gained during prototyping stages of the CH and SS1 solenoid R&D. The design is quite close to that of the SS1 solenoid, but a different type of superconducting strand is used and the longer main coil is made of two separate sections.

Below the operating current of ~200 A, quench protection can be arranged as was done in the case of the CH and SS1 systems. Above this current level, additional measures must be developed to ensure the desired (high) level of the device protection.

The next step of this R&D will be finishing design and building a prototype of the SS2 Type-2 solenoid, having in mind that Type-1 will be built the same way, but with the use of a dummy corrector insert. Meanwhile, the computational tool for study of quench protection must be modified to allow making more accurate and diverse analysis of various options of the solenoid quench protection.

References:

[1] G. Davis, et al, " HINS Linac SS-1 Section Prototype Focusing Solenoid Design", TD-08-010, FNAL, March 2008.

[2] R. Carcagno, et al, "Test Solenoid PDST03-0 Performance and Test Results", TD-06-029, FNAL, July 2006.

[3] T. Khabiboulline, I. Terechkine, "Superconducting Cavity Magnetic Field Requirements", TD-08-006, February 2008.

[4] G. Chlachidze, et al, "HINS_SS1_SOL_02d Fabrication Summary and Test Results", TD-09-001, FNAL, January 2009.

[5] I. Terechkine, "Quench Protection Study for the Focusing Solenoids of the Superconducting Sections of the HINS Linac", TD-09-002, February 2009.

[6] V. Veretennikov, I. Terechkine, "HINS Front End SS-1 Section Focusing Solenoid Quench Protection Analysis", FNAL TD-07-020, FNAL, TD, August 2007.

[7] I. Terechkine, V. Veretennikov, "Normal Zone Propagation in Superconducting Focusing Solenoids and Related Quench Protection Issues", IEEE Transaction on Applied Superconductivity, v. 18, NO. 2, pp. 1325 – 1328, June 2008.